Journal of Intelligent & Robotic Systems (2024) 110:132
https://doi.org/10.1007/s10846-024-02165-5

REGULAR PAPER

Neural Network-based Adaptive Finite-time Control for 2-DOF Helicopter Systems with Prescribed Performance and Input Saturation

Hui Bi[1] · Jian Zhang[2] · Xiaowei Wang[1] · Shuangyin Liu[3] · Zhijia Zhao[1] · Tao Zou[1]

Received: 4 November 2023 / Accepted: 20 August 2024

Abstract
In this study, we propose an adaptive neural network (NN) control approach for a 2-DOF helicopter system characterized by finite-time prescribed performance and input saturation. Initially, the NN is utilized to estimate the system's uncertainty. Subsequently, a novel performance function with finite-time attributes is formulated to ensure that the system's tracking error converges to a narrow margin within a predefined time span. Furthermore, adaptive parameters are integrated to address the inherent input saturation within the system. The boundedness of the system is then demonstrated through stability analysis employing the Lyapunov function. Finally, the effectiveness of the control strategy delineated in this investigation is validated through simulations and experiments.

Keywords Adaptive control · NN control · 2-DOF helicopter systems · Finite-time prescribed performance · Input saturation

1 Introduction

Helicopters are widely utilized in various fields such as transportation, logistics, freight forwarding, and geological surveys, primarily due to their distinct advantages of vertical takeoff and landing capabilities, hovering flight capability, and minimal takeoff requirements [1]. However, helicopters pose a challenging control problem due to their inherently nonlinear nature, multi-input, multi-output dynamics, and the presence of uncertainties and cross-coupling effects among their axes. These characteristics present substantial hurdles in the development of robust control systems for helicopters.

Researchers have proposed various control algorithms to address challenges such as uncertainty in helicopter dynamics. For instance, in [2], an accelerated feedback augmentation control was developed as a robust enhancement of the H_∞ algorithm, effectively mitigating uncertainties and external disturbances during UAV flight. In [3], an adaptive integral inversion method with an online uncertainty estimation algorithm was introduced for robust control of 3-DOF helicopters. However, with the rapid advancement of neural networks (NNs) in recent years, scholars have increasingly employed them in handling nonlinear systems. The rapid learning capability and localized approximation advantages of radial basis function NNs (RBFNNs) have led to their widespread use in nonlinear control applications [4]. In [5, 6], the authors devised an adaptive control scheme employing NNs to address uncertainties inherent in 3-DOF helicopter systems. In [7], the authors employed NNs to estimate unknown functions within the same system and validated the algorithm's efficacy through simulation. For 2-DOF helicopter systems afflicted by model uncertainty and

Jian Zhang, Xiaowei Wang, Shuangyin Liu, Zhijia Zhao, Tao Zou contributed equally to this work

✉ Xiaowei Wang
meewxw_ee@gzhu.edu.cn

Hui Bi
bihui2022@e.gzhu.edu.cn

Jian Zhang
zhangjian041715@163.com

Shuangyin Liu
shuangyinliu@zhku.edu.cn

Zhijia Zhao
zhjzhaoscut@163.com

Tao Zou
tzou@gzhu.edu.cn

[1] School of Mechanical and Electrical Engineering, Guangzhou University, Guangzhou 510006, China

[2] School of Automation Science and Engineering, South China University of Technology, Guangzhou 510640, China

[3] College of Information Science and Technology, Zhongkai University of Agriculture and Engineering, Guangzhou 510225, China

Published online: 07 September 2024

unknown backlash, deterministic learning strategies based on adaptive NNs were proposed by the authors in [8]. However, the literature reviewed primarily focuses on the convergence and steady-state behavior of the system. In practical engineering applications, it is crucial for the system to satisfy specific performance requirements, necessitating further investigation.

Recently, several control strategies have emerged to explore prescribed performance. For instance, in [9], the authors proposed a function to characterize performance, delineating constraints on tracking errors. They employed an error transformation technique to convert the constrained problem of tracking the trajectory of a robotic manipulator into an unconstrained stabilization problem. In [10], the authors introduced a prescribed performance function (PPF) with an error transformation to ensure that constraints satisfy the system's output requirements by transforming the constrained problem into an unconstrained one. Furthermore, in [11], the authors presented a control strategy utilizing neural networks to address performance constraints within the system, employing an adaptive prescribed performance approach. Additionally, in [12], researchers introduced a robust control strategy tailored for 3-DOF helicopter systems, with a focus on achieving prescribed transient and steady-state performance. While the PPF can manage both transient and steady-state constraints of the system, the aforementioned studies have concentrated on prescribed performance as time approaches infinity. However, some practical systems, such as unmanned aerial vehicles and robotic systems, necessitate achieving the desired performance and completing the control task within a finite time.

Finite-time control research has recently witnessed significant advancements, boasting a quicker convergence rate compared to asymptotic stability control, rendering it widely applicable across various practical systems. In [13], to tackle issues such as the sluggish convergence of the adaptive law attributed to the traditional gradient algorithm, thereby compromising system performance, the authors introduced finite-time convergence for adaptive NNs. In [14, 15], researchers devised finite-time control strategies employing adaptive NNs, aimed at addressing challenges encountered in diverse nonlinear systems, including issues pertaining to gradual convergence. Alongside finite-time convergence techniques, input saturation emerges as a prevalent phenomenon in real systems, posing a significant challenge and thereby paving the way for further research opportunities.

In practical engineering applications, the input of the system actuator often faces an upper limit, resulting in input saturation that is unavoidable. Input saturation constrains the system's performance and significantly impacts its stability [16]. Consequently, addressing the input saturation problem has become a focal point of current research. In [17–19], authors applied the Nussbaum gain technique to manage the nonlinearity caused by saturation in spacecraft or other nonlinear systems. Similarly, in [20, 21], the phenomenon of input saturation in robotic arms and helicopter systems was addressed by utilizing NNs to approximate the saturation error and developing adaptive NN controllers. Additionally, in [22], authors employed adaptive laws with multiplicative operation solutions to handle the saturation error term and devised an adaptive NN control strategy. Despite the availability of several treatment approaches for input saturation, there remains a dearth of studies considering finite-time control, prescribed performance, and input saturation simultaneously for 2-DOF helicopter systems. This research gap serves as a motivation for further investigation.

Based on the existing literature, this study proposes an adaptive finite time control (AFTC) strategy integrating NNs for 2-DOF helicopter systems. This approach is specifically designed to cope with the input saturation challenge and achieve the prescribed performance. The main contributions of this paper compared to previous literature are summarized below:

1) Unlike the PPF in [9–12], this study introduces a finite time performance function. This novel approach enables the system error to converge to a narrow zero domain within a finite time. Moreover, it facilitates the convergence of both NN weights and adaptive parameters within a finite time.
2) In contrast to [17–19], which employs the Nussbaum gain technique to address input saturation, this study proposes the use of adaptive parameters to tackle the input saturation problem. This approach avoids the high-frequency oscillatory characteristics associated with the Nussbaum function and the selection of controller parameters that can significantly affect system stability.
3) The controller proposed in this study not only ensures fast convergence of the system error within the specified performance region but also preserves the system's transient properties within the a priori bounds. Furthermore, all signals in the closed-loop system are semi-globally consistent and bounded, ensuring system stability.

2 Problem Formulation and Preliminaries

2.1 Problem Formulation

From [23], the dynamics model of the 2-DOF helicopter system can be deduced in the following

$$\ddot{\chi} = \frac{-M_o g_o l_o \cos\chi - D_{opp}\dot{\chi} - M_o l_o^2 \dot{\psi}^2 \sin\chi \cos\chi}{(J_{opp} + M_o l_o^2)}$$

$$+\frac{K_{opp}V_p+K_{opy}V_y}{(J_{opp}+M_o l_o^2)}, \tag{1}$$

$$\ddot{\psi}=\frac{-D_{oyy}\dot{\psi}+2M_o l_o^2\dot{\psi}\dot{\chi}\sin\chi\cos\chi}{(J_{oyy}+M_o l_o^2\cos^2\chi)}+\frac{K_{oyp}V_p+K_{oyy}V_y}{(J_{oyy}+M_o l_o^2\cos^2\chi)}, \tag{2}$$

where χ and ψ indicate the pitch and yaw angle. M_o is the weight of the helicopter system. l_o is the distance between the fixed frame of the helicopter and the center of mass. g_o denotes the gravitational acceleration. D_{opp} and D_{oyy} denote the coefficient of viscous friction. J_{opp} and J_{oyy} denote the moments of inertia. K_{opp}, K_{opy}, K_{oyy} and K_{oyp} denote the thrust torques [24].

Subsequently, a unique performance metric is suggested as follows.

Definition 1 ([25]) If the conditions outlined below are met by a continuous function $\zeta_i(t)$.

1) For any $t \le T_l$, there are $\lim_{t\to T_l}\zeta_i(t)=\zeta_{iT_l}$ and $\zeta_i(t)=\zeta_{iT_l}$ with ζ_{iT_l} and T_l being design parameter and setting time, respesctinely;
2) $\dot{\zeta}_i \le 0$;
3) $\zeta_i(t) > 0$.

Then, the function $\zeta_i(t)$ is denoted as the FTPF.

According to Definition 1, we apply the FTPF as follows.

$$\zeta_i(t)=\begin{cases}\bar{\zeta}_i(\zeta_{i0}-\frac{t}{T_l})e^{\lambda_i(1-\frac{T_l}{T_l-t})}+\zeta_{iT_l}, t\in[0,T_l]\\ \zeta_{iT_l}, t\in[T_l,+\infty]\end{cases} \tag{3}$$

where $\zeta_{i0}\ge 1$, $\bar{\zeta}_i > 0$, $\lambda_i > 0$, and $\zeta_{iT_l} > 0$ are design parameters.

Next, a transformation of error is suggested in the following manner.

$$T(z_{1i})=\frac{e^{z_{1i}}-e^{-z_{1i}}}{e^{z_{1i}}+e^{-z_{1i}}} \tag{4}$$

where z_1 is the transformed error.

Remark 1 We can find that i) the function (4) is a monotonically increasing function; ii) $T(z_{1i}) \in (-1,1)$; iii) $\lim_{z_{1i}\to+\infty}T(z_{1i})=1$ and $\lim_{z_{1i}\to-\infty}T(z_{1i})=-1$.

Define $r=[r_1,r_2]^T$, $r_1=[\chi,\psi]^T$, and $r_2=[\dot{\chi},\dot{\psi}]^T$.Referring to Eqs. 1 and 2, the transformation of the 2-DOF helicopter system model into the general form of a MIMO system is achievable.

$$\dot{r}_1=r_2, \tag{5}$$

$$\dot{r_2}=X(r)+\Delta X(r)+G(r)u, \tag{6}$$

$$y=r_1, \tag{7}$$

where $u=[V_p,V_y]^T$ is the control input of the system and also the output of saturation nonlinearity. $\Delta X(r)$ represent a unknown smooth nonlinear function. $X(r)$ and $G(r)$ are given as follows.

$$X(r)=\begin{bmatrix}\frac{-M_o g_o l_o\cos(r_{11})-D_{opp}r_{21}-M_o l_o^2 r_{22}^2\sin(r_{11})\cos(r_{11})}{J_{opp}+M_o l_o^2}\\ \frac{-D_{oyy}r_{22}+2M_o l_o^2 r_{22}r_{21}\sin(r_{11})\cos(r_{11})}{J_{oyy}+M_o l_o^2\cos^2(r_{11})}\end{bmatrix}, \tag{8}$$

$$G(r)=\begin{bmatrix}\frac{K_{opp}}{J_{opp}+M_o l_o^2} & \frac{K_{opy}}{J_{opp}+M_o l_o^2}\\ \frac{K_{oyp}}{J_{oyy}+M_o l_o^2\cos^2(r_{11})} & \frac{K_{oyy}}{J_{oyy}+M_o l_o^2\cos^2(r_{11})}\end{bmatrix}. \tag{9}$$

Moreover, the input saturation $u_i(t)$, $i=1,2$ is proposeed by

$$u(\mu_i(t))=\begin{cases}\bar{\mu}_i(t), \mu_i(t)>\bar{\mu}_i(t)\\ \mu_i(t), \underline{\mu}_i(t)\le\mu_i(t)\le\bar{\mu}_i(t)\\ \underline{\mu}_i(t), \mu_i(t)<\underline{\mu}_i(t)\end{cases} \tag{10}$$

where $\mu_i(t)$ denotes the controler variable to be design later. $\bar{\mu}_i(t)$ and $\underline{\mu}_i(t)$ are the upper and the lower of the control input.

The control input can be represented as

$$u(\mu(t))=\mu(t)+\Delta(\mu) \tag{11}$$

where $\mu=[\mu_1,\mu_2]^T$ and the saturation error $\Delta(\mu)=[\Delta(\mu_1),\Delta(\mu_2)]^T$ is given as

$$\Delta(\mu_i)=\begin{cases}\bar{\mu}_i-\mu_i, \mu_i>\bar{\mu}_i\\ 0, \underline{\mu}_i\le\mu_i\le\bar{\mu}_i\\ \mu_i-\underline{\mu}_i, \mu_i<\underline{\mu}_i\end{cases} \tag{12}$$

Then, substituting (11) into (6), we have

$$\dot{r}_2=X(r)+\Delta X(r)+G(r)\mu+d^* \tag{13}$$

where $d^*=G\Delta(\mu)$.

2.2 Preliminaries

Assumption 1 [26] *There exists an unknown constant $\bar{G}>0$ such that it satisfies $||G(r)||\le\bar{G}$.*

Assumption 2 [27] *The input saturation error $\Delta(\mu)$ is bound and satisfies $||\Delta(\mu)|| \leq \bar{\Delta}$ with $\bar{\Delta} > 0$ being a constant.*

Lemma 1 [28] *In this study, the RBFNN is used to approximate the unknown continuous function $f(K) : R^n \rightarrow R$:*

$$f(K) = W^T D(K) \tag{14}$$

where $K \in R^n$ and n denote the input of the NN and its dimension, respectively. $W = [w_1, w_2, \ldots, w_{N_0}]^T$ is the weight vector of the NN. $D(K) = [D_1(K), D_2(K), \ldots, D_{N_0}(K)]^T$ represents the basis function.

Due to its very strong approximation ability, the RBFNN is able to approximate any function on a tight set to arbitrary accuracy as follows

$$f(K) = W^{*T} D(K) + \delta(K) \tag{15}$$

where W^* indicates the ideal weight vector. $\delta(K)$ is the approximation error of the NN and satisfies $||\delta(K)|| \leq \bar{\delta}$ with $\bar{\delta}$ being a small positive constant.

Lemma 2 [29] *For any $z \in R$ and $c > 0$, the subsequent inequality is valid.*

$$|z| - z\tanh(\frac{z}{c}) \leq 0.2785c \tag{16}$$

3 Controller Design and Stability Analysis

The objective of the control strategy in this study is to ensure that the helicopter's output closely follows the desired trajectory motion and that the system's error converges to a region near zero within a finite amount of time during the control process. Furthermore, the uncertainty in the system is addressed using a NN-based approach, while the issue of input saturation is managed using an adaptive parameter system. The flowchart of the algorithm is depicted in Fig. 1.

Let us define the tracking error

$$e_1 = r_1 - r_d \tag{17}$$

where r_d is the desired trajectory.

To simplify the controller design, we suggest the error transformations outlined below.

$$e_{1i} = \zeta_i(t) T(z_{1i}) \tag{18}$$

Based on Eq. 4, the transformed error is converted as

$$z_{1i} = \frac{1}{2}\log\frac{\zeta_i(t) + e_{1i}(t)}{\zeta_i(t) - e_{1i}(t)} \tag{19}$$

The time derivative of z_1 yields

$$\dot{z}_{1i} = \frac{\zeta_i(t)\dot{e}_{1i} - \dot{\zeta}_i(t)e_{1i}(t)}{2[\zeta_i^2(t) - e_{1i}^2(t)]} \tag{20}$$

Define $z_1 = [z_{11}, z_{12}]^T$, we can rewrite (20) as

$$\dot{z}_1 = \frac{1}{2}S\dot{e}_1 - \frac{1}{2}SQe_1 \tag{21}$$

where $S = \text{diag}\{s_i\}$, $s_i = \frac{\zeta_i(t)}{[\zeta_i^2(t) - e_{1i}^2(t)]}$, $i = 1, 2$ and $Q = \text{diag}\{\frac{\dot{\zeta}_1(t)}{\zeta_1(t)}, \frac{\dot{\zeta}_2(t)}{\zeta_2(t)}\}$.

Next, we define the coordinate transformation as follows.

$$\theta_1 = z_1 \tag{22}$$

$$\theta_2 = r_2 - \alpha \tag{23}$$

with α is a virtual controller.

Considering the Lyapunov function as

$$V_1 = \frac{1}{2}\theta_1^T\theta_1 \tag{24}$$

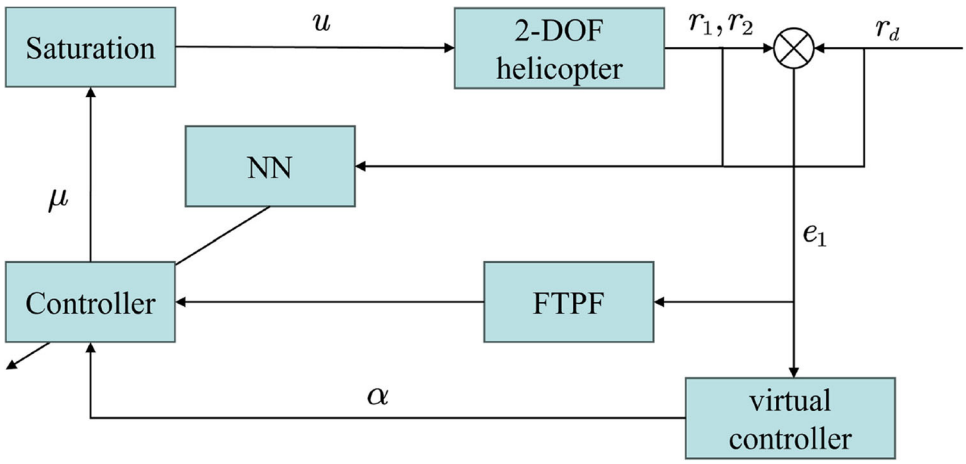

Fig. 1 Control scheme design figure

Substituting (21) and (22) into the time derivative of V_1 yields

$$\begin{aligned}\dot{V}_1 &= \theta_1^T \dot{\theta}_1 \\ &= \frac{1}{2}\theta_1^T \left(S\dot{e}_1 - SQe_1\right) \\ &= \frac{1}{2}\theta_1^T S(\theta_2 + \alpha - \dot{r}_d - Qe_1)\end{aligned} \tag{25}$$

The virtual controller is selected as

$$\alpha = -c_1\theta_1 + \dot{r}_d + Qe_1(t) \tag{26}$$

where c_1 is a design parameter.

Substituting (26) into (25), we have

$$\dot{V}_1 = -\frac{1}{2}c_1\theta_1^T S\theta_1 + \frac{1}{2}\theta_1^T S\theta_2 \tag{27}$$

As $\Delta X(r)$ represents an unidentified smooth nonlinear function, the RBFNN can be employed to approximate it.

$$\Delta X(r) = W^{*T} D(K) + \delta(K) \tag{28}$$

where $K = [r_1^T, r_2^T, r_d^T, \dot{r}_d^T]^T$ represents the input vector of the NN. $\delta(K)$ signifies the approximation error associated with the NN and adheres to the condition $||\delta(K)|| \leq \bar{\delta}$ with $\bar{\delta} > 0$ is an unknown constant.

According to Assumption 1 and 3, it is known that d^* is bounded such that satisfies $||d^*|| \leq d$. We define $\tilde{W} = \hat{W} - W^*$ and $\tilde{d} = \hat{d} - d$. Set $\hat{W}$ and $\hat{d}$ to be the estimates of W^* and d, respectively.

Putting (13) and (28) into the time derivative of Eq. 23, we have

$$\dot{\theta}_2 = X(r) + W^{*T} D(K) + \delta(K) + G(r)\mu + d^* - \dot{\alpha} \tag{29}$$

Then, we develop NN-based adaptive finite-time controller as follows:

$$\begin{aligned}\mu = -G^{-1}(X(r) + \hat{W}^T D(K) + \hat{d}\tanh(\frac{\theta_2}{c}) \\ + \frac{1}{2}S\theta_1 + c_2\theta_2 - \dot{\alpha})\end{aligned} \tag{30}$$

where c_2 is a positive constant.

Next, we design the adaptive updating rates for $\hat{W}$ and $\hat{d}$ as follows

$$\dot{\hat{W}} = \Gamma_1(D(k)\theta_2^T - \gamma_1\hat{W}), \tag{31}$$

$$\dot{\hat{d}} = \Gamma_2(\theta_2^T \tanh(\frac{\theta_2}{c}) - \gamma_2\hat{d}) \tag{32}$$

where $\Gamma_1 = \Gamma_1^T \in R^{2\times 2}$ is a diagonal matrixand the elements within the matrix are all positive constants. Γ_2, γ_1, γ_2, and c are the design parameters.

Remark 2 Because of $\lim_{t\to T_f^+}[\frac{\partial^2\zeta_i(t)}{\partial t^2}] = \lim_{t\to T_f^-}[\frac{\partial^2\zeta_i(t)}{\partial t^2}] = 0$, the FTPF is twice differentiable. This also yields the terms $\dot{\zeta}_i$, $\ddot{\zeta}_i$ and α. For a detailed proof refer to [25].

Theorem 1 *Consider the existence of finite-time prescribed performance and input saturation for 2-DOF helicopter systems* (1) *and* (2)*. An NN-based adaptive finite-time controller* (30) *is proposed and the corresponding update rate* (31)*, and* (32) *is designed. The developed NN-based AFTC strategy ensures the boundedness of the closed-loop system without violating the finite-time prescribed performance in* Eq. 3.

Proof Construct the following Lyapunov function:

$$V_2 = V_1 + \frac{1}{2}\theta_2^T\theta_2 + \frac{1}{2}\text{tr}\{\tilde{W}^T\Gamma_1^{-1}\tilde{W}\} + \frac{1}{2\Gamma_2}\tilde{d}^2 \tag{33}$$

The time derivative of V_2 yields

$$\dot{V}_2 = \dot{V}_1 + \theta_2^T\dot{\theta}_2 + \text{tr}\{\tilde{W}^T\Gamma_1^{-1}\dot{\hat{W}}\} + \frac{1}{\Gamma_2}\tilde{d}\dot{\hat{d}} \tag{34}$$

Substituting (30) into (29), we have

$$\begin{aligned}\theta_2^T\dot{\theta}_2 &= \theta_2^T(X(r) + W^{*T}D(K) + \delta(K) + G(r)v + d^* \\ &\quad - \dot{\alpha}) \\ &= -\theta_2^T\tilde{W}^T D(K) + e_2^T\delta(K) + \theta_2^T d^* - \theta_2^T\hat{d}\tanh(\frac{\theta_2}{c}) \\ &\quad - \frac{1}{2}\theta_2^T S\theta_1 - c_2\theta_2^T\theta_2\end{aligned} \tag{35}$$

Then, inserting (27) and (35) into (34), we get

$$\begin{aligned}\dot{V}_2 &= -\frac{1}{2}c_1\theta_1^T S\theta_1 + \frac{1}{2}\theta_1^T S\theta_2 - \theta_2^T\tilde{W}^T D(K) + e_2^T\delta(K) \\ &\quad + \theta_2^T d^* - \theta_2^T\hat{d}\tanh(\frac{\theta_2}{c}) - \frac{1}{2}\theta_2^T S\theta_1 - c_2\theta_2^T\theta_2 \\ &\quad + \text{tr}\{\tilde{W}^T\Gamma_1^{-1}\dot{\hat{W}}\} + \frac{1}{\Gamma_2}\tilde{d}\dot{\hat{d}}\end{aligned} \tag{36}$$

Since d^* is bounded such that satisfies $||d^*|| \leq d$, and

$$\theta_2^T d^* \leq d\sum_{i=1}^{2}|\theta_{2i}| \tag{37}$$

In addition, we can obtain the following conversion

$$d\theta_2^T\tanh(\frac{\theta_2}{c}) = d\sum_{i=1}^{2}(\theta_{2i}\tanh(\frac{\theta_{2i}}{c})) \tag{38}$$

Table 1 System paramaters [26]

Symbol	Value	Unit	Symbol	Value	Unit
J_{opp}	0.0215	kg·m^2	l_o	0.0071	m
J_{oyy}	0.0237	kg·m^2	K_{opp}	0.022	N·m/V
M_o	1.0750	kg	K_{opy}	0.0221	N·m/V
D_{opp}	0.0071	N/V	K_{oyp}	−0.0227	N·m/V
D_{oyy}	0.0220	N/V	K_{oyy}	0.0022	N·m/V
g_o	9.8	m/s^2			

According to Lemma 2, the ensuing inequality can be derived

$$d\sum_{i=1}^{2}|\theta_{2i}| - d\sum_{i=1}^{2}(\theta_{2i}\tanh(\frac{\theta_{2i}}{c})) \le 0.557cd \tag{39}$$

Substituting (31)- (32) and (37)- (39) into Eq. 36, we have

$$\begin{aligned}\dot{V}_2 &= -\frac{1}{2}c_1\theta_1^T S\theta_1 - c_2\theta_2^T\theta_2 - \theta_2^T\tilde{W}^T D(K) + \theta_2^T\delta(K)\\ &+ \theta_2^T d^* - d\theta_2^T\tanh(\frac{\theta_2}{c}) - \tilde{d}\theta_2^T\tanh(\frac{\theta_2}{c})\\ &+ \mathrm{tr}\{\tilde{W}^T(D(k)\theta_2^T - \gamma_1\hat{W})\} + \tilde{d}(\theta_2^T\tanh(\frac{\theta_2}{c}) - \gamma_2\hat{d})\\ &\le -\frac{1}{2}c_1\theta_1^T S\theta_1 - c_2\theta_2^T\theta_2 + \theta_2^T\delta(K) + a_0\iota\\ &+ 0.557cd - \mathrm{tr}\{\gamma_1\tilde{W}^T\hat{W}\} - \gamma_2\tilde{d}\hat{d}\end{aligned} \tag{40}$$

Utilizing Young's inequality, we obtain

$$-\mathrm{tr}\{\gamma_1\tilde{W}^T\hat{W}\} \le -\frac{\gamma_1}{2}||\tilde{W}||_F^2 + \frac{\gamma_1}{2}||W^*||_F^2 \tag{41}$$

$$\theta_2^T\delta(K) \le \frac{1}{2}\theta_2^T\theta_2 + \frac{1}{2}\bar{\delta}^2 \tag{42}$$

$$-\gamma_2\tilde{d}\hat{d} \le -\frac{1}{2}\gamma_2\tilde{d}^2 + \frac{1}{2}\gamma_2 d^2 \tag{43}$$

Inserting (41)- (43) into (40), we have

$$\begin{aligned}\dot{V}_2 &\le -\frac{1}{2}c_1\theta_1^T S\theta_1 - (c_2 - \frac{1}{2})\theta_2^T\theta_2 - \frac{\gamma_1}{2}||\tilde{W}||_F^2\\ &- \frac{1}{2}\gamma_2\tilde{d}^2 + \frac{1}{2}\bar{\delta}^2 + 0.557cd + \frac{\gamma_1}{2}||W^*||_F^2 + \frac{1}{2}\gamma_2 d^2\end{aligned} \tag{44}$$

From Eqs. 3 and 4, it is clear that $0 < \zeta_{iT_l} \le \zeta_i \le \zeta_i(0)$. Thus, we can known that $\frac{1}{\zeta_i(0)} \le \frac{1}{\zeta_i} \le s_i = \frac{\zeta_i(t)}{[\zeta_i^2(t) - e_{1i}^2(t)]}$. Let $\Xi = \mathrm{diag}\{\frac{1}{\zeta_i(0)}\}$, $i = 1, 2$, Eq. 44 can be rewritten as

$$\begin{aligned}\dot{V}_2 &\le -\frac{1}{2}c_1\theta_1^T\Xi\theta_1 - (c_2 - \frac{1}{2})\theta_2^T\theta_2 - \frac{\gamma_1}{2}||\tilde{W}||_F^2\\ &- \frac{1}{2}\gamma_2\tilde{d}^2 + \frac{1}{2}\bar{\delta}^2 + 0.557cd + \frac{\gamma_1}{2}||W^*||_F^2 + \frac{1}{2}\gamma_2 d^2\\ &\le -\kappa V_2 + L\end{aligned} \tag{45}$$

where

$$\kappa = \min\{c_1\lambda_{\min}(\Xi), 2(c_2 - \frac{1}{2}), \frac{\gamma_1}{\lambda_{\max}(\Gamma_1^{-1})}, \Gamma_2\gamma_2\} \tag{46}$$

and

$$L = \frac{1}{2}\bar{\delta}^2 + 0.557cd + \frac{\gamma_1}{2}||W^*||_F^2 + \frac{1}{2}\gamma_2 d^2 \tag{47}$$

For all the signals in the system to be bounded, the conditions that should be satisfied by c_1, c_2, γ_1, Γ_1, Γ_2, γ_2 are shown below

$$\begin{aligned}&c_1 > 0, \lambda_{\min}(\Xi), c_2 - \frac{1}{2} > 0, \gamma_1 > 0,\\ &\lambda_{\max}(\Gamma_1^{-1}) > 0, \Gamma_2\gamma_2 > 0\end{aligned} \tag{48}$$

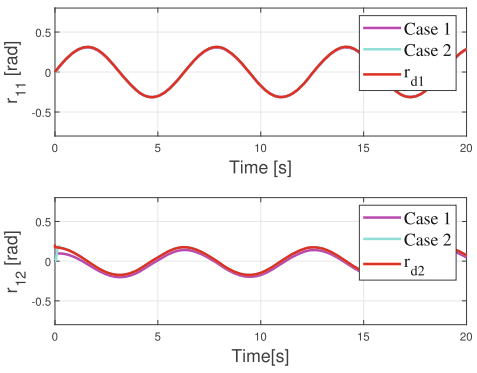

(a) Tracking performance.

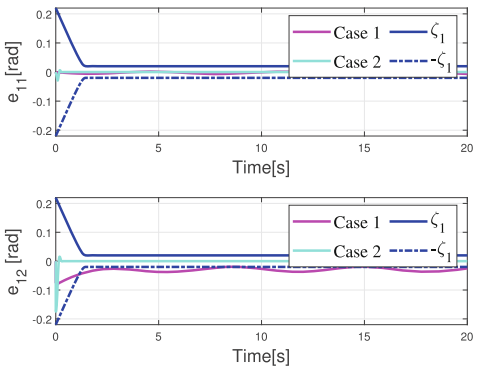

(b) Tracking errors.

Fig. 2 Comparison of the control performance of Case 1 and 2

According to Lemma 2 and Eq. 44, we obtain

$$0 \leq V_2 \leq \frac{L}{\kappa} + [V_2(0) - \frac{L}{\kappa}]e^{-\kappa t} \tag{49}$$

From which we have $\lim_{t\to\infty} V_2 = \frac{L}{\kappa}$. That is, V_2 is convergent. As a result, the signals θ_1, θ_2, $\tilde{W}$, $\tilde{\rho}$, and $\tilde{d}$ are all bounded. From Eq. 19, the steady state error can be calculated as

$$\lim_{t\to T_l} |z_{1i}| \leq \Lambda_i \tag{50}$$

where $\Lambda_i = \frac{e^f-1}{e^f+1}\zeta_{iT_l}$, with $f = \sqrt{8V_0 + 8\frac{L}{\kappa}}$. It is clear that $\Lambda_i < \zeta_{iT_l}$ can be obtained by the definition of Λ_i. Hence, the

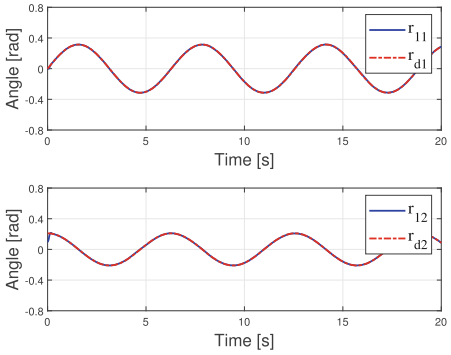

(a) Tracking performance.

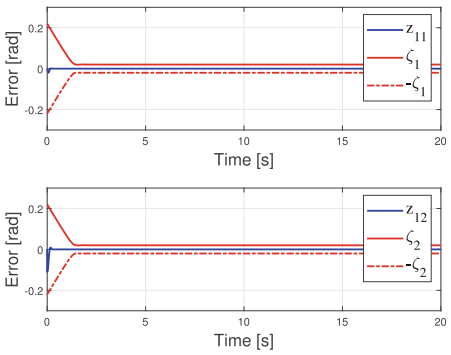

(b) Tracking errors.

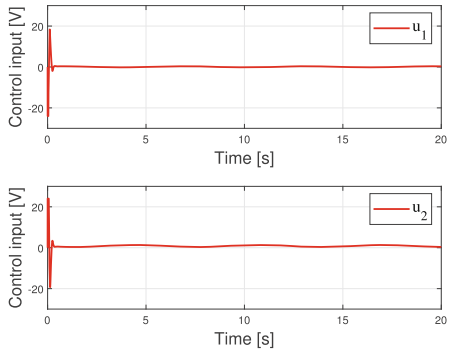

(c) Control input.

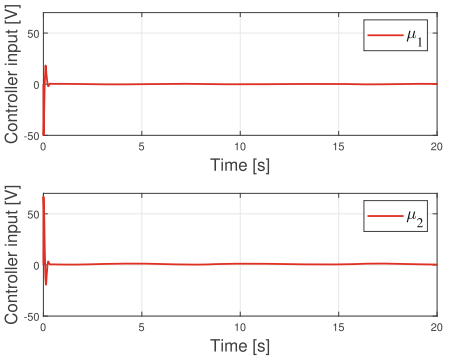

(d) Controller input.

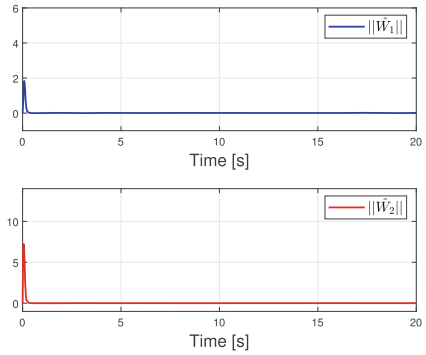

(e) Weights $||\hat{W}_1||$ and $||\hat{W}_2||$ of the NNs.

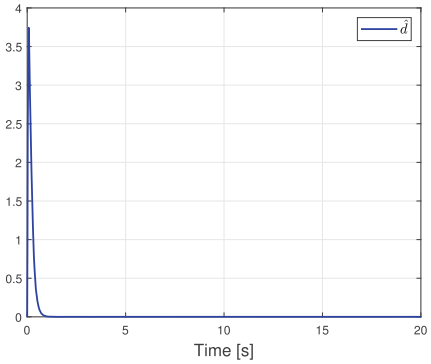

(f) Adapyive parameter $\hat{d}$.

Fig. 3 The control performance of Case 2

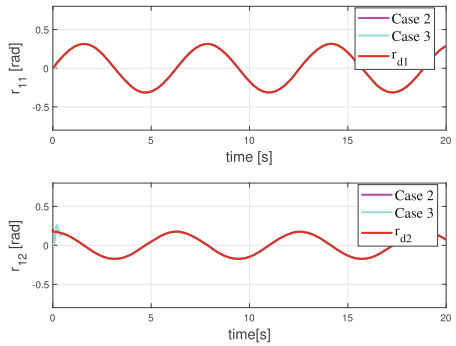

(a) Tracking performance.

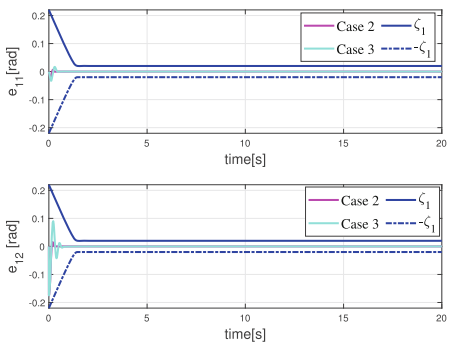

(b) Tracking errors.

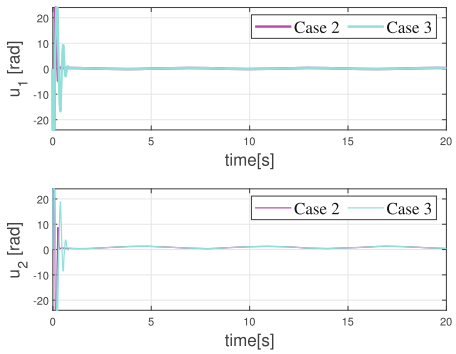

(c) Control input.

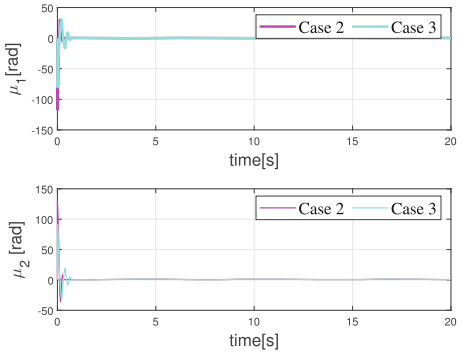

(d) Controller input.

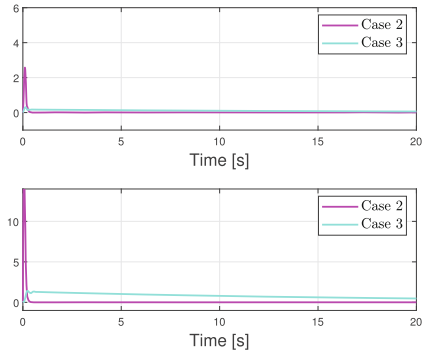

(e) Weights $||\hat{W}_1||$ and $||\hat{W}_2||$ of the NNs.

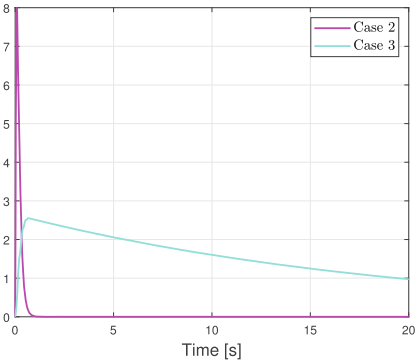

(f) Adapyive parameter $\hat{d}$.

Fig. 4 Comparison of the control performance of Case 2 and 3

tracking error e_1 converges within a specified region. This concludes the proof. □

Remark 3 This research introduces an adaptive finite-time NN for 2-DOF helicopters with prescribed performance and input saturation. The approach can offer direction for 4-DOF helicopter control, even if it cannot be directly extended to other nonlinear systems like 4-DOF and 6-DOF helicopter systems. Our next research path will be to apply the control approach developed in this study to 4-DOF helicopter systems. Furthermore, this study suggests a new FTPF that permits the system's error, NN weights, and adaptive parameters to converge in finite time, in contrast to [9–12]. Unlike [17–19], this study uses adaptive parameters to compensate for saturation error. This avoids the high-frequency oscillatory characteristics associated with the Nussbaum function, as well as the selection of controller parameters, which can significantly affect the system's stability.

4 Simulation Results

Simulations are employed to validate the efficacy of the AFTC strategy based on NNs proposed in this study. The parameters for the 2-DOF helicopter system are provided in Table 1. The system's initial trajectory is set as $r_1(0) = [0, 0]^T$. The specified trajectory is denoted by $r_d = [\frac{\pi}{10}\sin(t), \frac{\pi}{18}\cos(t)]^T$. The initial value for the NN weight is set to zero. The design parameters of the system are $c_1 = 10$, $c_2 = 10$, $\Gamma_1 = 32I_{128\times128}$, $\Gamma_2 = 15$, $\gamma_1 = 0.5$, $\gamma_2 = 0.5$, and $c = 0, 1$. The FTPF parapeters are choose as $\zeta_{i0} = 1$, $\bar{\zeta}_i = 0.2$, $\lambda_i = 0.2$, $T_l = 1.5$, and $\zeta_{iT_l} = 0.02$. The upper and lower of the input saturation are $\bar{\mu}_i = 24$ and $\underline{\mu}_i = -24$, respectively.

4.1 Case 1: Proportional-Differential (PD) Control

In this case, we formulate a PD controller for comparison with the control strategy introduced in this investigation. The PD controller is structured as follows:

$$v = -K_p e_1 - K_d \dot{e}_1 \tag{51}$$

where K_p and K_d denote the proportional and differential gains with $K_p = \text{diag}\{30, 30\}$ and $K_d = \text{diag}\{40, 40\}$.

Figure 2(a) shows the output tracking response, while Fig. 2(b) illustrates the error trajectory. As depicted in Fig. 2, the system error in the PD controller fails to converge in finite time and exceeds the specified performance constraints, resulting in decreased system stability.

4.2 Case 2: Under the Proposed Control

The effectiveness of the controller suggested in Eq. 30 is affirmed through this case study. Figure 3(a) displays the tracking of the system output trajectory, while Fig. 3(b) illustrates that the system error remains confined within the specified region. Figure 3(c) and (d) illustrate the system's control input and controller input, respectively. Additionally, Fig. 3(e) and (f) depict the trajectories of the NN weights and adaptive parameters, showcasing their semi-global finite-time stabilization. The results clearly indicate that our suggested control strategy effectively resolves the saturation phenomenon in the system and rapidly constrains the system error within the prescribed range.

4.3 Case 3: Under the Proposed Control without Finite-Time

In this case, we consider a prescribed performance function without finite time based on the controller design of this study. The specific form of the prescribed performance function we use has been given in [30]. The simulation results are shown in Case 3 of Fig. 4. Figure 4(a) and (b) represent the output trajectory and error of the system, respectively. Figure 4(c) and (d) represent the control inputs of the system and the inputs of the controller, respectively. Figure 4(e) represents the paradigm of NN weights. Figure 4(f) represents the convergence trajectory of the adaptive parameters.

Based on Fig. 4(b), (e), and (f), we observe that the control strategy proposed in this case, compared to the one discussed in this paper, can ensure that the system's error remains within the constraints of the prescribed performance and converges to a smaller region. It also enables the convergence of the

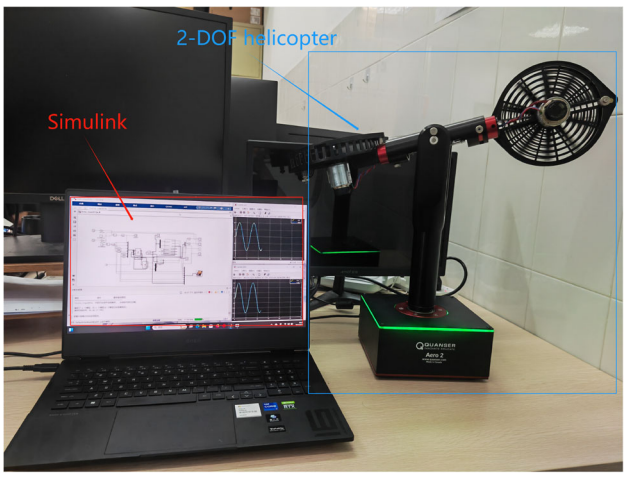

Fig. 5 Helicopter platform

NN weights and the adaptive parameters. However, it does not guarantee their convergence in a finite time.

5 Experimental Results

We carry out experimental validation on Quanser's 2-DOF helicopter platform, depicted in Fig. 5, to substantiate the effectiveness and superiority of the control strategy proposed in this study.

5.1 Scheme 1: Under the Proposed Control

The prescribed trajectory is $r_d = [\frac{\pi}{18}\sin(t), \frac{\pi}{12}\sin(t)]^T$. Implementing the control algorithm suggested in this research experimentally produced outcomes, as illustrated in Fig. 6(a)-(d). Figure 6(a) and (b) portray the reaction of the output variables as they track the intended trajectory, while Fig. 6(c) demonstrates the tracking error. Figure 6(d) reveals the control input. These figures corroborate that the system's tracking error can be limited to the prescribed region within a finite time without violating any constraints.

5.2 Scheme 2: Under the Proposed Control without Finite-Time

To substantiate the superiority of the advanced control strategy suggested, comparative experiments are carried out. These experiments specifically address the stipulated performance constraints and input saturation, with no consideration for finite-time control. The prescribed performance constraints are based on the methodology described in [30]. The desired trajectory is $r_d = [\frac{\pi}{18}\sin(t), \frac{\pi}{12}\sin(t)]^T$. Figure 7(a) exhibits the response of the system's output variables as they track the specified trajectory, while Fig. 7(b) and (c) display the system's tracking error. Additionally, Fig. 7(d) presents

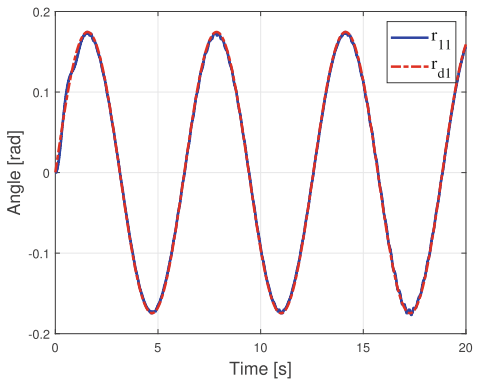

(a) Tracking performance r_{11}.

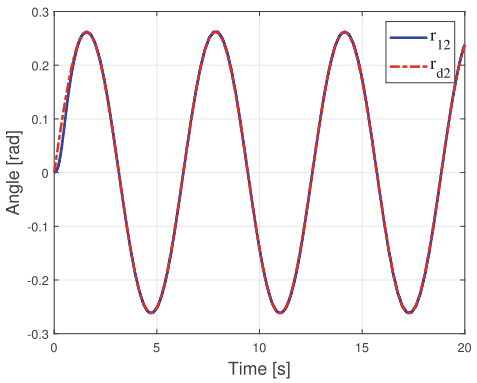

(b) Tracking performance r_{12}.

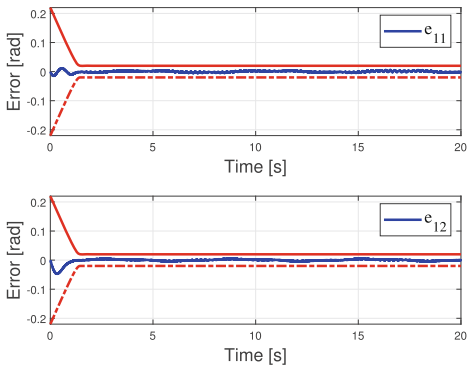

(c) Tracking errors.

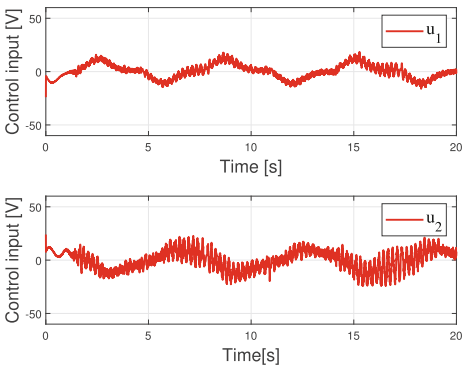

(d) Control input.

Fig. 6 The control performance of Scheme 1

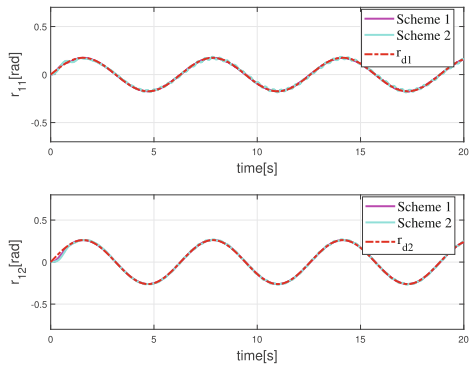

(a) Tracking performance.

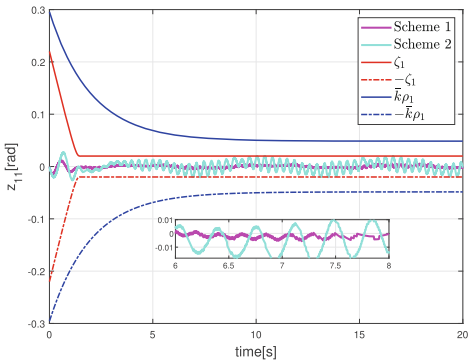

(b) Tracking error e_{11}.

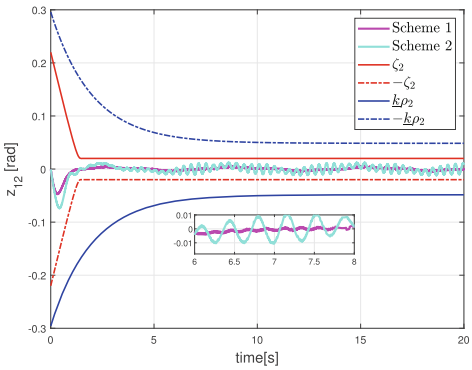

(c) Tracking error e_{12}.

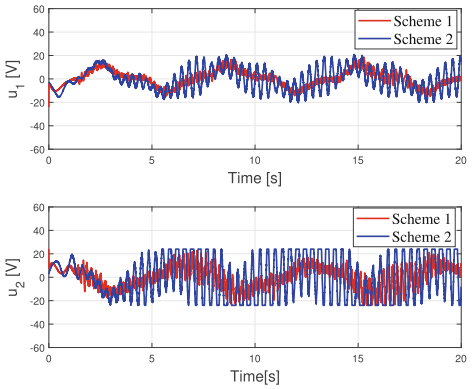

(d) Control input.

Fig. 7 Comparison of the control performance of Scheme 1 and 2

the control inputs to the system. Notably, Fig. 7(b) and (c) highlight that without considering finite time control, the system error converges slower and oscillates in a narrower region, thus leading to a less stable system.

5.3 Scheme 3: Under the Proposed Control without Saturation Compensation

In this scheme, we examine a control algorithm that does not account for input saturation compensation. The control parameters utilized in this algorithm remain consistent with those in Scheme 1. Figure 8(a) illustrates the output tracking trajectory of the system, while Fig. 8(b) and (c) depict the tracking error of the system, and Fig. 8(d) represents the system's input. In comparison to the control strategy advocated in this paper, the method proposed in this scheme exhibits a larger error and fails to address input saturation, resulting in diminished input performance of the system. These circumstances contribute to the deterioration of system stability and may even cause damage to system components under severe conditions. Consequently, the control strategy proposeded in this paper substantially enhances system stability and robustness.

6 Conclusion

In this study, an AFTC approach utilizing NNs was introduced to tackle both prescribed performance and input saturation challenges in the 2-DOF helicopter system. The NNs were served the purpose of approximating the system's uncertainty term. To guarantee a rapid convergence of the tracking error within the specified performance region in finite time, an enhanced FTPF was suggested. An adaptive parameter was incorporated to manage the impact of input saturation. The effectiveness and superiority of the proposed

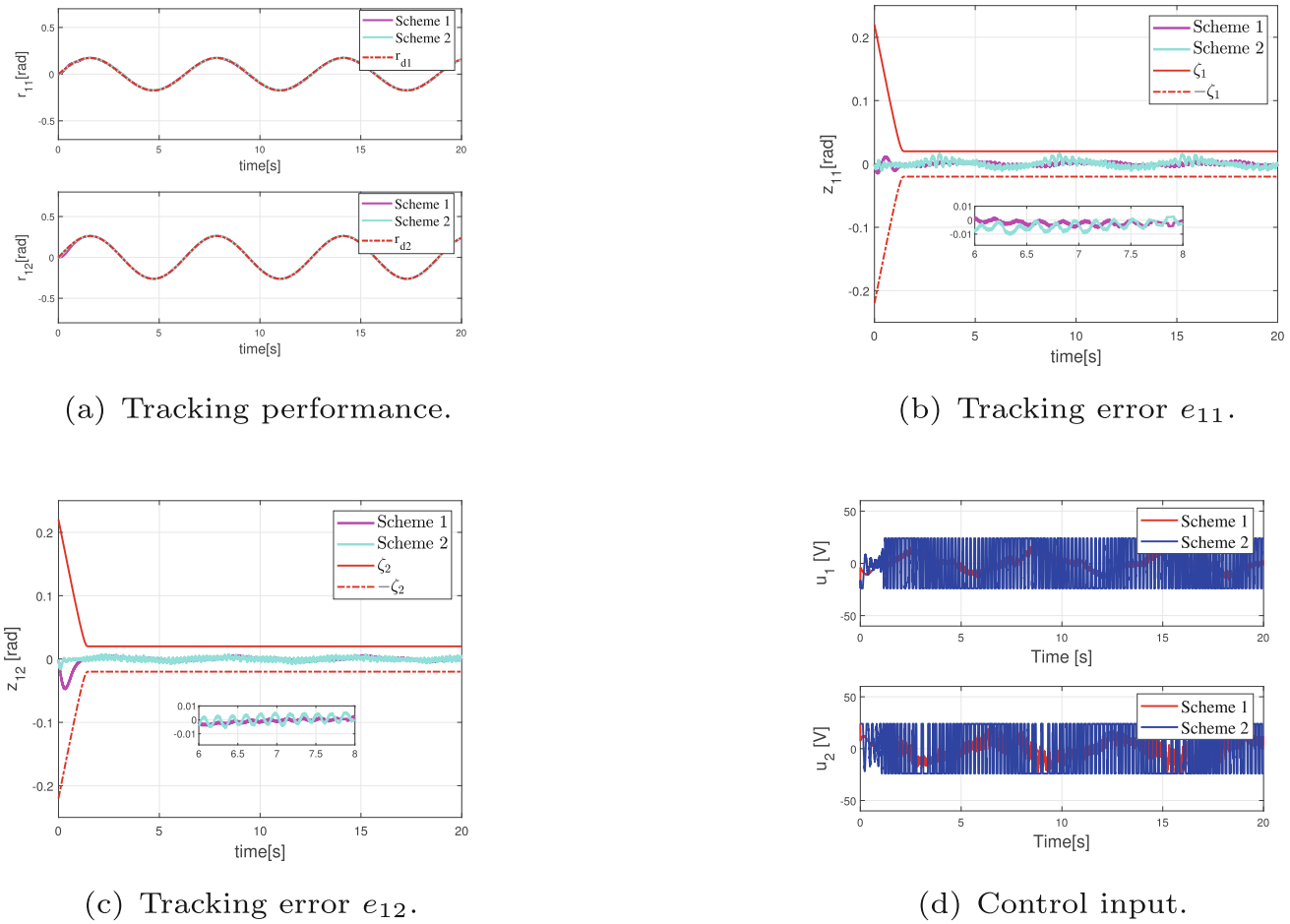

(a) Tracking performance.

(b) Tracking error e_{11}.

(c) Tracking error e_{12}.

(d) Control input.

Fig. 8 Comparison of the control performance of Scheme 1 and 3

control strategy were confirmed by a combination of simulations and experiments.

Author Contributions All authors contributed to the study conception and design. Hui Bi—Conceptulization, Methdology, Software, Data curation, Writing-original draft. Jian Zhang—Software, Data curation, Methdology, Writing-original draft. XiaoWei Wang—Supervision, investigation, data curation. Shuangyin Liu— investigation, Supervision. Zhijie Zhao—resources, project administration. Tao Zou—validation, investigation.

Funding This work was supported in part by the National Natural Science Foundation of China under Grant 62373390, in part by the Guangdong Basic and Applied Basic Research Foundation under Grant 2023B1515120018, 2023B1515120019 and 2022B1515120059, in part by the Science and Technology Planning Project of Guangzhou, China under Grant 2023A03J0120, and in part by the Guangdong-Hong Kong-Macao Key Laboratory of Multi-scale Information Fusion and Collaborative Optimization Control of Complex Manufacturing Process.

Data Availability The datasets used or analyzed during the current study are available from the corresponding author on reasonable request.

Code Availability The datasets used or analyzed during the current study are available from the corresponding author on reasonable request.

Declarations

Competing Interests The authors have no relevant financial or nonfinancial interests to disclose.

References

1. Zhao, Z., He, W., Zou, T., Zhang, T., Chen, C.L.P.: Adaptive broad learning neural network for fault-tolerant control of 2-dof helicopter systems. IEEE Transactions on Systems, Man, and Cybernetics: Systems, pp 1–11 (2023). https://doi.org/10.1109/TSMC.2023.3299303
2. He, Y., Han, J.: Acceleration-feedback-enhanced robust control of an unmanned helicopter. J. Guid. Control. Dyn. **33**(4), 1236–1250 (2010). https://doi.org/10.2514/1.45659
3. Fang, Z., Gao, W., Zhang, L.: Robust adaptive integral backstepping control of a 3-dof helicopter. Int. J. Adv. Rob. Syst. **9**(3), 79 (2012). https://doi.org/10.5772/50864
4. Jiang, B., Liu, D., Karimi, H.R., Li, B.: Rbf neural network sliding mode control for passification of nonlinear time-varying delay systems with application to offshore cranes. Sensors **22**(14), 5253 (2022). https://doi.org/10.3390/s22145253
5. Chen, Y., Yang, X., Zheng, X.: Adaptive neural control of a 3-dof helicopter with unknown time delay. Neurocomputing **307**, 98–105 (2018). https://doi.org/10.1016/j.neucom.2018.04.041
6. Yang, X., Zheng, X.: Adaptive nn backstepping control design for a 3-dof helicopter: theory and experiments. IEEE Trans. Industr. Electron. **67**(5), 3967–3979 (2020). https://doi.org/10.1109/TIE.2019.2921296
7. Wang, Y., Yang, J., Yang, X., Wang, T.: Adaptive neural network-based fault-tolerant control for a three degrees of freedom helicopter. Int. J. Control **96**(1), 182–190 (2023). https://doi.org/10.1080/00207179.2021.1984583
8. Zhao, Z., He, W., Zhang, F., Wang, C., Hong, K.-S.: Deterministic learning from adaptive neural network control for a 2-dof helicopter system with unknown backlash and model uncertainty. IEEE Trans. Industr. Electron. **70**(9), 9379–9389 (2023). https://doi.org/10.1109/TIE.2022.3213916
9. Wang, M., Yang, A.: Dynamic learning from adaptive neural control of robot manipulators with prescribed performance. IEEE Transactions on Systems, Man, and Cybernetics: Systems **47**(8), 2244–2255 (2017). https://doi.org/10.1109/TSMC.2016.2645942
10. Zerari, N., Chemachema, M.: Robust adaptive neural network prescribed performance control for uncertain cstr system with input nonlinearities and external disturbance. Neural Comput. Appl. **32**(14), 10541–10554 (2020). https://doi.org/10.1007/s00521-019-04591-1
11. Li, Y., Tong, S.: Adaptive neural networks prescribed performance control design for switched interconnected uncertain nonlinear systems. IEEE Transactions on Neural Networks and Learning Systems **29**(7), 3059–3068 (2018). https://doi.org/10.1109/TNNLS.2017.2712698
12. Verginis, C.K., Bechlioulis, C.P., Soldatos, A.G., Tsipianitis, D.: Robust trajectory tracking control for uncertain 3-dof helicopters with prescribed performance. IEEE/ASME Trans. Mechatron. **27**(5), 3559–3569 (2022). https://doi.org/10.1109/TMECH.2021.3136046
13. Luan, F., Na, J., Huang, Y., Gao, G.: Adaptive neural network control for robotic manipulators with guaranteed finite-time convergence. Neurocomputing **337**, 153–164 (2019). https://doi.org/10.1016/j.neucom.2019.01.063
14. Wang, Y., Zhang, J., Zhang, H., Xie, X.: Finite-time adaptive neural control for nonstrict-feedback stochastic nonlinear systems with input delay and output constraints. Appl. Math. Comput. **393**, 125756 (2021). https://doi.org/10.1016/j.amc.2020.125756
15. Liu, M., Ji, R., Ge, S.S., Fellow, I.: Adaptive neural control for a tilting quadcopter with finite-time convergence. Neural Comput. Appl. **33**(23), 15987–16004 (2021). https://doi.org/10.1007/s00521-021-06215-z
16. Qin, J., Du, J., Li, J.: Adaptive finite-time trajectory tracking event-triggered control scheme for underactuated surface vessels subject to input saturation. IEEE Trans. Intell. Transp. Syst. **24**(8), 8809–8819 (2023). https://doi.org/10.1109/TITS.2023.3256094
17. Yan, K., Chen, M., Wu, Q., Wang, Y., Zhu, R.: Prescribed performance fault tolerant control for uncertain nonlinear systems with input saturation. Int. J. Syst. Sci. **51**(2), 258–274 (2020). https://doi.org/10.1080/00207721.2019.1703058
18. Hu, Q., Shao, X., Guo, L.: Adaptive fault-tolerant attitude tracking control of spacecraft with prescribed performance. IEEE/ASME Trans. Mechatron. **23**(1), 331–341 (2018). https://doi.org/10.1109/TMECH.2017.2775626
19. Yu, J., Shi, P., Lin, C., Yu, H.: Adaptive neural command filtering control for nonlinear mimo systems with saturation input and unknown control direction. IEEE Transactions on Cybernetics **50**(6), 2536–2545 (2020). https://doi.org/10.1109/TCYB.2019.2901250
20. He, W., Sun, Y., Yan, Z., Yang, C., Li, Z., Kaynak, O.: Disturbance observer-based neural network control of cooperative multiple manipulators with input saturation. IEEE Transactions on Neural Networks and Learning Systems **31**(5), 1735–1746 (2020). https://doi.org/10.1109/TNNLS.2019.2923241
21. Zhang, J., Yang, Y., Zhao, Z., Hong, K.-S.: Adaptive neural network control of a 2-dof helicopter system with input saturation. Int. J. Control Autom. Syst. **21**(1), 318–327 (2023). https://doi.org/10.1007/s12555-021-1011-2
22. Ma, Z., Huang, P.: Adaptive neural-network controller for an uncertain rigid manipulator with input saturation and full-order state constraint. IEEE Transactions on Cybernetics **52**(5), 2907–2915 (2022). https://doi.org/10.1109/TCYB.2020.3022084
23. Zhao, Z., He, W., Mu, C., Zou, T., Hong, K.-S., Li, H.-X.: Reinforcement learning control for a 2-dof helicopter with state constraints: Theory and experiments. IEEE Transactions on Automation Science and Engineering, pp 1–11 (2022). https://doi.org/10.1109/TASE.2022.3215738
24. Inc., Q.: Quanser aero laboratory guide. Tech. Rep. Quanser (2016)
25. Zeng, Q., Zhao, J.: Event-triggered adaptive finite-time control for active suspension systems with prescribed performance. IEEE Trans. Industr. Inf. **18**(11), 7761–7769 (2022). https://doi.org/10.1109/TII.2021.3139002
26. Zhao, Z., Zhang, J., Chen, S., He, W., Hong, K.-S.: Neural-network-based adaptive finite-time control for a two-degree-of-freedom helicopter system with an event-triggering mechanism. IEEE/CAA Journal of Automatica Sinica **10**(8), 1754–1765 (2023). https://doi.org/10.1109/JAS.2023.123453
27. Cao, S., Sun, L., Jiang, J., Zuo, Z.: Reinforcement learning-based fixed-time trajectory tracking control for uncertain robotic manipulators with input saturation. IEEE Transactions on Neural Networks and Learning Systems **34**(8), 4584–4595 (2023). https://doi.org/10.1109/TNNLS.2021.3116713
28. Zhu, C., Jiang, Y., Yang, C.: Fixed-time neural control of robot manipulator with global stability and guaranteed transient performance. IEEE Trans. Industr. Electron. **70**(1), 803–812 (2023). https://doi.org/10.1109/TIE.2022.3156037
29. Kong, L., Lai, Q., Ouyang, Y., Li, Q., Zhang, S.: Neural learning control of a robotic manipulator with finite-time convergence in the presence of unknown backlash-like hysteresis. IEEE Transactions on Systems, Man, and Cybernetics: Systems **52**(3), 1916–1927 (2022). https://doi.org/10.1109/TSMC.2020.3034757
30. Guo, Q., Zhang, Y., Celler, B.G., Su, S.W.: Neural adaptive backstepping control of a robotic manipulator with prescribed performance constraint. IEEE Transactions on Neural Networks and Learning Systems **30**(12), 3572–3583 (2019). https://doi.org/10.1109/TNNLS.2018.2854699

Hui Bi received the B.Eng. degree from North University of China, Taiyuan, China, in 2010, and the M.Eng. degree from Guangdong University of Technology, Guangzhou, China, in 2013. He is currently working toward the Ph.D. degree majoring in operations research and control theory with the Guangzhou University , Guangzhou, China. His research interests include unmanned control technology and robotics.

Jian Zhang received the B.Eng. degree from West Anhui University, Luan, China, in 2020, and the M.Eng. degree from Guangzhou University, Guangzhou, China, in 2023. He is currently working toward the Ph.D. degree in control science and engineering with the South China University of Technology, Guangzhou, China. His research interests include demonstration learning, and robotics.

Xiaowei Wang received his M.S. degree in 2006, and his Ph.D. degree in 2014, from the Institute of Electrical Engineering, Harbin Institute of Technology, Harbin, China. He entered a postdoctoral workstation in the Shenzhen Academy of Aerospace Technology, China, from 2014 to 2016. He is currently a lecturer with the School of Mechanical and Electrical Engineering, Guangzhou University. His research interests include electric machine, power electronics, and control systems.

Shuangyin Liu received the Ph.D. degree from the College of Information and Electrical Engineering, China Agricultural University, in 2014. He is currently a Professor with the College of Information Science and Technology, Zhongkai University of Agriculture and Engineering. His current research interests are in the areas of intelligent information system of agriculture, artificial intelligence, big data, software engineering, and computational intelligence.

Zhijia Zhao received the B.Eng. degree in automatic control from the North China University of Water Resources and Electric Power, Zhengzhou, China, in 2010, and the M.Eng. and Ph.D. degrees in automatic control from the South China University of Technology, Guangzhou, China, in 2013 and 2017, respectively. He is currently a Professor with the School of Mechanical and Electrical Engineering, Guangzhou University, Guangzhou. His research interests include adaptive and learning control, flexible mechanical systems, and robotics.

Tao Zou was born in Liaoning, China in 1975. He received the Ph.D. degree in control theory and control engineering in 2005 from Shanghai Jiao Tong University, Shanghai, China. Since 2019, he has been a professor in the School of Mechanical and Electrical Engineering, Guangzhou University. His research interests include industrial process modeling and simulation, model predictive control, advanced process control, decision making and real-time optimization technology research and application.